ORIGINAL PAPER

Conformation and tautomerizm of the 2-methyl-4-pyridin-2′-yl-1,5-benzodiazepine molecule. An ab initio study

Nurten Tezer

Abstract The protomeric tautomerizm and conformation of the 2-methyl-4-pyridin-2′-yl-1,5-benzodiazepine molecule were investigated, and its three neutral tautomers (B_1, B_2,B_3) and their rotamers (C_1,C_2,C_3) were considered. Full geometry optimizations were carried out at the HF/6-31G* and B3LYP/6-31G* levels in gas phase and in water. The tautomerization processes in water ($\varepsilon=78.54$) were studied by using self-consistent reaction field theory. The calculation showed that the boat conformation is dominant for the seven-membered diazepine ring in all of the structures, even with different double bond positions. The calculated relative free energies (ΔG) showed that the tautomer C_1 was the most stable structure, and its conformer B_1 was the second most stable in the gas phase and in water.

Keywords Ab initio · 1,5-Benzodiazepine · Tautomerizm

Introduction

Benzodiazepines (BZD) usually occur in diimine form A rather than in the conjugated vinamidine forms depicted in formulas A-I and A-II . In diimine form A some extra stabilization arises from the conjugation of the imine groups with the benzene ring. Cyclic conjugation as in A-I and A-II may indeed lead to destabilization of the molecules because

N. Tezer (✉)
Faculty of Arts and Science, Chemistry Department,
Cumhuriyet University,
58140 Sivas, Turkey
e-mail: ntezer@cumhuriyet.edu.tr

it involves interaction of 12 π-electrons around the periphery of the molecules as implied in A-I, or of 8 π-electrons around the seven-membered ring as in A-II; either of these configurations destabilize 4n π-electron systems [1].

A   A-I   A-II
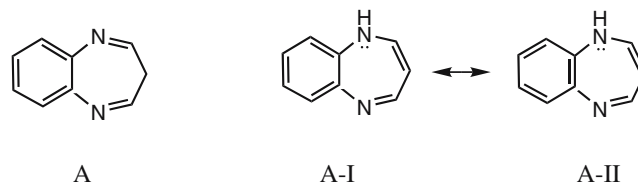
Benzodiazepine derivatives are well-described heterocycles as they have found applications as an important class of therapeutic agents. BZDs and their annelated derivatives exhibit a wide spectrum of biological activities and have found applications in pharmaceutical chemistry [2–6]. Some BZD derivatives are used as dyes for acrylic fibers [7] in photography. In addition, 1,5-BZDs are valuable synthons for the preparation of other fused ring compounds [8–10] such as triazolo-, oxadiazolo-, oxazino-and furano-BZD. Due to their wide range of applications, these compounds have received a great deal of attention in connection with their synthesis [11–17]. Experimental and clinical evidence has suggested that BZDs could also influence immune cell properties such as phagocyte activity, chemotaxis and the production of superoxide ions and cytokines, either by reducing stress and anxiety status or through stimulation of peripheral BZD receptors [18–20]. Despite their wide range of pharmacological activities, and industrial and synthetic applications, theoretical studies of 1,5-BZDs have received

little attention. Recently, Tjiou and co-workers published an NMR study and synthesis of 1,5-BZD derivatives [21]. They showed anisochrony between methylene hydrogens. In their NMR measures, the Hb signal shows a coupling that disappears upon irradiation of the N-1H signal at 15.5 ppm. No such coupling is observed on the signal of Ha. In the same paper, it was announced that another example of strongly anisochronous methylene hydrogens was found in 2-methyl-4-pyridin-2′-yl-1,5-benzodiazepine **B**. This compound has three tautomeric forms: **B₁**, **B₂**, and **B₃**. NMR observations indicated a very small participation of the tautomers **B₂** and **B₃**.

Because structural data for the structures of **A** are lacking, theoretical computations have been performed to examine these geometries as well as the energies of the **A** and **B**, **C** forms. Theoretical investigation represents a practical means of obtaining information about the energetics of tautomers. The present work describes the structural and energetic features of these tautomeric forms in the gas phase and in water using ab initio and density functional theory (DFT) calculations. Tautomeric equilibrium transition structure energies in the gas phase were also investigated.

Methods

The ab initio and DFT calculations were performed using the Gaussian 03 W package [22] The geometries were optimized at the HF and B3LYP computational level with the 6-31G* basis set in the gas phase and in water. The transition structure for tautomers and rotameric conversions ($A_1 \rightarrow A_2$, $B_1 \rightarrow B_2$, $B_1 \rightarrow B_3$, $B_1 \rightarrow C_1$, $C_1 \rightarrow C_2$, $C_1 \rightarrow C_3$) were also at the B3LYP level in the gas phase. Harmonic vibrational frequencies were also calculated at both levels of theory in order to characterize the stationary points as local minima (equilibrium structures) or first-order saddle points (transition structures) on the potential energy surface and to evaluate the zero-point vibrational energy (ZPE). All transition structures were characterized with only one imaginary vibrational frequency. Force calculations at the equilibrium geometries yielded only real frequencies. The atomic charges were calculated using the Mulliken population analysis included in the Gaussian 03 W package. The solute–solvent interaction was evaluated using the self-consistent reaction field (SCRF) method, which is based on Onsager's reaction field theory of electrostatic solvation [23]. The reaction field calculation was carried out for
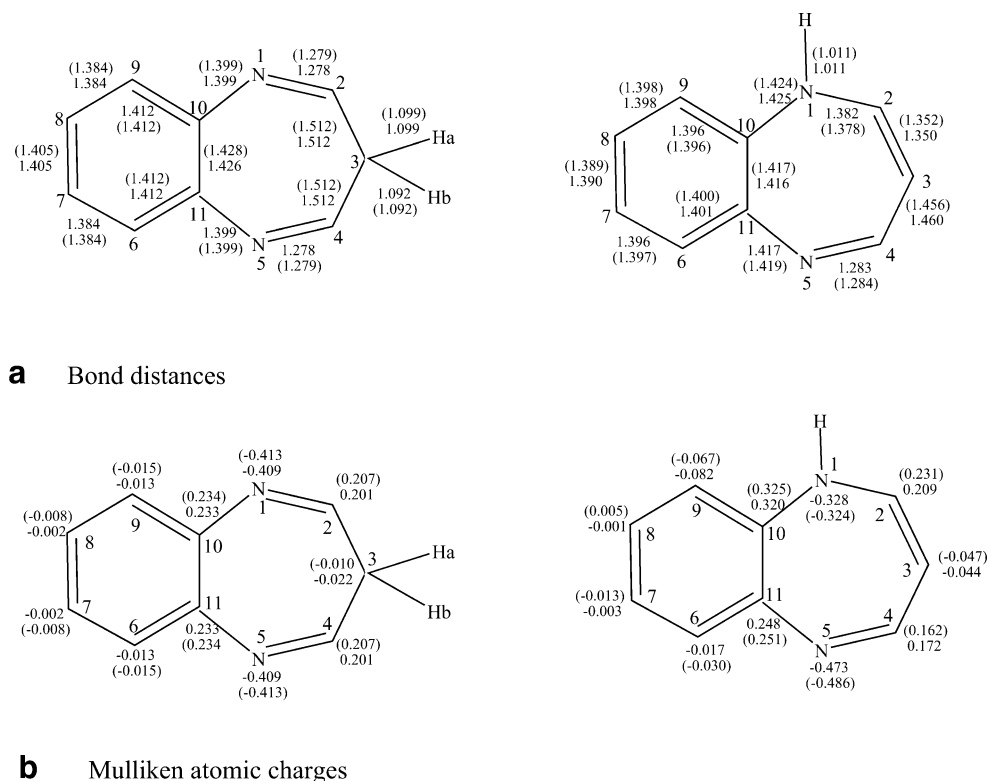
Scheme 1 Tautomer and rotamer structures of the main compounds and the numbering system used in this article
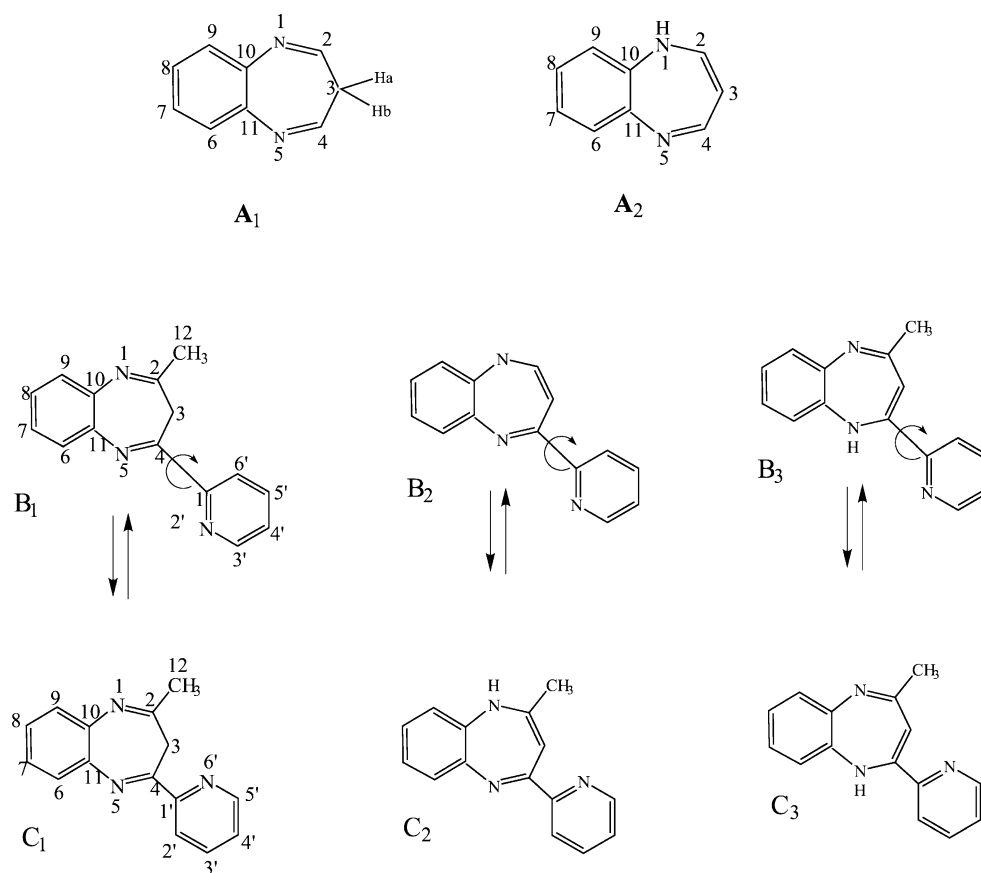
Table 1 Selected B3LYP/6-31G* geometrical parameters for tautomer and rotamers in the gas phase and in water. Distances in Å; angles in degrees. For numbering of atoms see Scheme 1

Parameter	ε=1						ε=78.54					
	B_1	B_2	B_3	C_1	C_2	C_3	B_1	B_2	B_3	C_1	C_2	C_3
$C_{10}C_{11}$	1.428	1.413	1.413	1.428	1.414	1.413	1.428	1.414	1.414	1.428	1.415	1.413
$C_{10}N_1$	1.397	1.427	1.412	1.397	1.422	1.409	1.397	1.425	1.412	1.397	1.422	1.410
N_1C_2	1.283	1.399	1.287	1.284	1.399	1.289	1.284	1.399	1.289	1.284	1.397	1.290
C_2C_3	1.517	1.352	1.469	1.517	1.352	1.468	1.518	1.353	1.466	1.516	1.353	1.464
C_3C_4	1.520	1.471	1.359	1.511	1.463	1.353	1.520	1.469	1.359	1.513	1.461	1.355
C_4N_5	1.285	1.287	1.387	1.289	1.293	1.400	1.286	1.288	1.388	1.289	1.293	1.398
N_5C_{11}	1.391	1.404	1.422	1.392	1.404	1.424	1.390	1.405	1.418	1.392	1.405	1.423
$C_4C_{1'}$	1.495	1.505	1.495	1.489	1.504	1.490	1.495	1.505	1.496	1.488	1.505	1.491
C_3Ha	1.099	1.085	1.084	1.098	1.081	1.084	1.098	1.085	1.083	1.098	1.081	1.084
C_3Hb	1.091	–	–	1.089	–	–	1.090	–	–	1.089	–	–
$N_{1,5} H$	–	1.013	1.017	–	1.012	1.010	–	1.013	1.019	–	1.012	1.011
$N_1C_2C_3$	121.76	123.04	128.94	121.95	124.12	128.47	121.72	122.95	129.23	122.02	124.14	128.94
$C_2C_3C_4$	106.52	125.42	125.30	105.28	125.53	125.08	106.26	125.41	125.28	105.23	125.53	125.28
$C_3C_4N_5$	120.79	128.45	123.73	122.24	129.02	122.13	120.52	128.59	123.68	122.07	129.17	122.37
$C_3C_4C_{1'}$	120.67	115.83	122.50	119.41	115.81	120.56	120.73	115.67	122.85	119.23	115.81	120.50
C_2C_3Ha	108.71	117.35	115.60	109.13	117.98	117.70	108.83	117.24	115.67	109.23	117.91	117.69
C_2C_3Hb	112.36	–	–	112.21	–	–	112.28	–	–	112.18	–	–
HaC_3Hb	108.18	–	–	110.30	–	–	108.13	–	–	110.37	–	–
HN_1C_2	–	112.92	–	–	113.00	–	–	112.93	–	–	113.09	–
HN_5C_4	–	–	110.18	–	–	114.72	–	–	109.64	–	–	114.58
$N_5C_4C_{1'}N_{2'}$	16.82	33.11	8.52	-174.64	-176.12	155.82	13.35	33.28	8.00	-173.27	-175.45	155.30
$C_3C_4C_{1'}N_{2'}$	-163.76	-147.78	-173.87	4.20	4.23	-23.32	-167.25	-147.86	-174.40	5.61	5.01	-23.34
$C_3C_4N_5C_{11}$	-4.48	4.91	41.96	-5.50	-5.80	-49.25	-4.50	5.04	41.61	-5.38	-5.92	-47.28
$C_{10}C_{11}N_5C_4$	-37.38	-34.24	-48.91	-36.49	31.66	53.58	-37.87	-34.61	-48.74	-36.82	31.51	52.38
$C_{11}C_{10}N_1C_2$	37.91	51.77	33.16	38.74	-48.71	-34.83	38.02	51.53	33.36	38.60	-48.35	-34.33
$N_1C_2C_3C_4$	-69.27	-5.84	-30.89	-69.12	6.23	33.07	-69.74	-6.61	-30.70	-69.41	6.49	32.16
$C_{10}N_1C_2C_3$	4.02	-47.51	-5.61	4.20	43.49	3.82	4.02	-49.93	-5.93	4.36	42.92	4.52
$C_2C_3C_4N_5$	69.19	30.86	9.64	69.78	-27.85	-6.61	69.65	31.27	9.87	69.89	-27.70	-7.32
$C_3C_4N_5C_{11}$	-4.48	4.91	41.96	-5.50	-5.80	-49.25	-4.49	5.04	41.61	-5.38	-5.92	-47.28

Fig. 1 Line drawings of structures A_1 and A_2 at the B3LYP/ 6-31G* level, illustrating the atom numbering scheme with the non-H atom labeling optimized bond distances in angstroms (**a**), and atomic charges (**b**), in the gas phase and in water. Values in water are in given in parentheses

a Bond distances

b Mulliken atomic charges

water ($\varepsilon = 78.54$). The cavity radius values (a_o) of structures were determined using the volume=tight option implemented in Gaussian 03 W.

Results and discussion

The tautomer and rotamer structures of the main compounds and the numbering system used throughout in this article are shown in Scheme 1. A_1 and A_2 shows BZD tautomers. The terms B_1, B_2, B_3 have been used to denote tautomer forms of **B** and C_1, C_2, C_3 used for their rotamers. The selected structural parameters B3LYP/6-31G* optimized geometries are listed in Table 1. Bond distances are given in angstroms and bond angles in degrees. Due to the size of the systems under investigation, complete optimizations of the geometrical structures required considerable computational effort. Therefore the geometry optimizations

Fig. 2 Optimized gas phase geometries at the B3LYP/ 6-31G* level
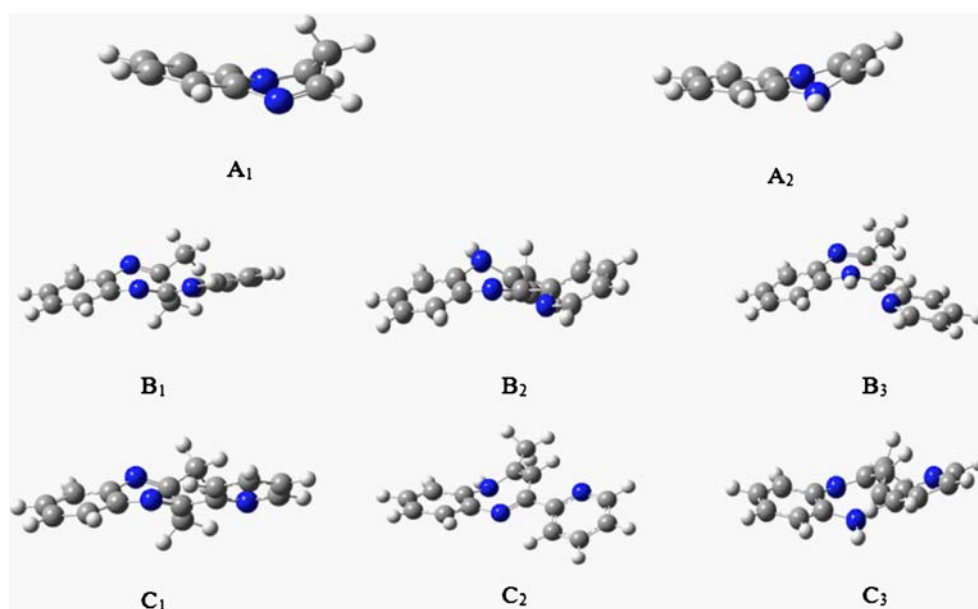
Table 2 Some Mulliken charges of tautomers calculated at the B3LYP/6-31G* level

	B_1	B_2	B_3	C_1	C_2	C_3
$\varepsilon=1$						
N_1	−0.474	−0.367	−0.531	−0.477	−0.376	−0.526
C_2	0.318	0.349	0.312	0.310	0.358	0.305
C_3	−0.084	−0.125	−0.144	−0.046	−0.083	−0.078
C_4	0.259	0.260	0.332	0.275	0.282	0.308
N_5	−0.466	−0.514	−0.375	−0.523	−0.597	−0.401
C_{10}	0.238	0.285	0.249	0.241	0.298	0.255
C_{11}	0.238	0.253	0.295	0.250	0.269	0.293
$\varepsilon=78.54$						
N_1	−0.478	−0.362	−0.546	−0.483	−0.374	−0.541
C_2	0.318	0.349	0.314	0.309	0.359	0.308
C_3	−0.075	−0.124	−0.139	−0.422	−0.085	−0.085
C_4	0.263	0.263	0.330	0.275	0.283	0.312
N_5	−0.473	−0.522	−0.373	−0.522	−0.601	−0.397
C_{10}	0.240	0.287	0.254	0.242	0.300	0.257
C_{11}	0.240	0.256	0.296	0.251	0.269	0.295

were performed at the HF/6-31G* and B3LYP/6-31G* levels. Calculated HF/6-31G* and B3LYP/6-31G* geometries showed that improved electron correlation had little effect on any of the calculated geometric parameters. In this regard, only B3LYP/6-31G* optimized structures all of species in the gas phase and in water are discussed.

Geometries

Figure 1a shows line-drawings of the structures A_1 and A_2, illustrating the atom numbering scheme with the non-H atom labeling and B3LYP/6-31G* optimized bond distances in angstroms; Fig. 1b shows Mulliken atomic charges. The most stable conformations predicted by ab initio computations at the B3LYP/6-31G* level are shown in Fig. 2. These geometries were drawn using Gauss View 3.0 [24].

The seven-membered diazepine ring (atoms $C_{10}C_{11}N_5C_4$/ $C_{11}C_{10}N_1C_2$) adopts a boat conformation. The internal

torsion angles of the ring were −37.68°($\varepsilon=1$), −38.03° ($\varepsilon=78.54$) ;37.68°($\varepsilon=1$), 38.03°($\varepsilon=78.54$) for A_1 and −28.54°($\varepsilon=1$) , −27.10°($\varepsilon=78.54$); 39.99°($\varepsilon=1$) , 37.61° ($\varepsilon=78.54$) for A_2. The boat conformation was predominantly observed for the seven-membered ring of BZD and its tautomers, even with different double bond positions and widely differing substituents [25, 26]. In the diazepine ring, the imine bonds N_1–C_2 and N_5–C_4 were clearly shorter than the amino bonds N_5–C_{11}/ N_1–C_{10}/N_1–C_2 . The methylene hydrogens exhibited anisochrony. The C_3–Ha bond was longer the C_3–Hb bond by 0.007 Å in the gas phase and in water. This anisochrony was also pointed out recently by Tjiou and co-workers [21]. In their NMR study, the ^{13}C spectrum at 20°C showed only sharp signals, in particular one at 35 ppm due to a CH_2 carbon identified with the DEPT-135 sequence. At the same time, the ^{1}H spectrum had a very large signal around 3.5 ppm. On lowering the temperature to 60°C in acetone, the ^{13}C signal at 35 ppm remained sharp, whereas the broad signal in the ^{1}H spectrum splits into two doublets (J=10.4 Hz) at 5.224 and 1.842 ppm. The high field doublet may be assigned to the hydrogen Ha, which is in the shielding areas of the two double bonds N_1–C_2 and C_4–N_5 and also of the aromatic ring of the BZD.

Analysis of calculation results showed that, on going from gas phase to water, there was almost no change in the bond lengths of the tautomer A_1. Unlike A_1, tautomer A_2 showed slight bond length changes. Only the N_1–C_2 and C_3–C_4 bonds were 0.004 Å longer in the gas phase than in water. Comparing BZD to its N-H form (NH-BZD), it can be seen that tautomerization especially affected the N_5–C_4, N_5–C_{11}, C_3–C_4, C_{10}–N_1 and aromatic ring bond lengths (Fig. 1).

In BZD, the N_5–C_4, N_5–C_{11}, N_1–C_{10} bonds were shorter than in NH-BZD, whereas the C_3–C_4, C_{10}–C_{11} and aromatic ring bonds were longer in the gas phase and in water. These data are an indication of the delocalization around the $C_3C_4N_5$ in NH-BZD and $C_2N_1C_{10}$, $C_4N_5C_{11}$ skeletons in BZD. An inspection of the $C_3C_4N_5C_{11}$ angle revealed that the out-of-plane deformation of the nitrogen

Table 3 Calculated total (hartree) energies in the gas phase and in water

Species	$\varepsilon=1$		$\varepsilon=78.54$	
	HF/6-31G*	B3LYP/6-31G*	HF/6-31G*	B3LYP/6-31G*
A_1	−454.340998	−457.247840	−454.342126	−457.248578
A_2	−454.329711	−457.237359	−454331664	−457.239237
TS(A_1→A_2)		−456.968107		
B_1	−738.925315	−743.662962	−738.927478	−743.664866
B_2	−738.913529	−743.650179	−738.915512	−743.652197
B_3	−738.922970	−743.662135	−738.926256	−743.665217
TS(B_1→B_2)		−743.277521		

Table 4 Calculated relative stabilities (in kcal mol^{-1}) for the tautomeric and rotameric forms of species shown in Fig. 1

Species	$\epsilon=1$		$\epsilon=78.54$	
	HF/6-31G*	B3LYP/6-31G*	HF/6-31G*	B3LYP/6-31G*
A_1	0.00	0.00	0.00	0.00
A_2	7.08	6.58	6.56	5.86
TS($A_1 \rightarrow A_2$)		175.54		
B_1	8.68	8.38	8.03	7.76
B_2	16.07	16.41	15.54	15.71
B_3	10.15	8.90	8.80	7.54
TS($B_1 \rightarrow B_2$)		250.25		
TS($B_1 \rightarrow B_3$)		248.27		
TS($C_1 \rightarrow B_1$)		166.41		
C_1	0.00	0.00	0.00	0.00
C_2	10.16	9.89	10.74	10.27
C_3	13.33	13.12	12.21	12.18
TS($C_1 \rightarrow C_2$)		243.10		
TS($C_1 \rightarrow C_3$)		247.06		
TS($B_2 \rightarrow C_2$)		174.15		
TS($B_3 \rightarrow C_3$)		173.19		
B_1	8.68	8.38	8.03	7.76
C_1	0.00	0.00	0.00	0.00
B_2	5.92	6.52	4.79	5.43
C_2	0.00	0.00	0.00	0.00
B_3	0.00	0.00	0.00	0.00
C_3	3.18	4.22	3.42	4.65

atom in BZD was quite different from that calculated in NH-BZD. In the aromatic benzene ring, C_{10}–C_{11} (also belonging to seven-membered ring) bond length was longer than C_{10}–C_9 and C_{11}–C_6 bonds in A_1 and A_2. These results showed that π-electrons of the benzene ring were

conjugated with imine groups of the seven-membered diazepine ring.

The calculations showed that the boat conformation was dominant for the seven-membered ring of BZD for all the other tautomers. Computer generated drawings of these

Table 5 Calculated zero-point vibrational energy (ZPE), thermal correction (H−H_0), ΔG^a and dipole moment at the B3LYP/6-31G* level in the gas phase and in water[b]

Species	$\epsilon=1$					$\epsilon=78.54$				
	H-H_0	ZPE	ΔG	μ(D)	ΔS	H-H_0	ZPE	ΔG	μ(D)	ΔS
A_1	4.89	95.37	0.00	2.08	0.00	4.89	95.36	0.00	2.54	0.00
A_2	5.12	95.45	6.22	3.31	−2.25	5.13	95.46	5.47	4.18	−2.38
TS($A_1 \rightarrow A_2$)	5.17	91.15	79.32	1.33	−3.78					
B_1	8.74	156.27	8.18	3.86	−0.16	8.75	156.25	7.38	5.58	−0.77
B_2	8.94	156.25	15.92	4.23	−1.68	8.93	156.24	15.21	5.50	−1.73
B_3	8.91	156.44	8.51	4.96	−1.97	8.89	156.45	7.18	7.20	−1.83
C_1	8.74	156.43	0.00	2.56	0.00	8.73	156.42	0.00	3.93	0.00
C_2	8.92	156.46	9.61	1.45	−1.65	8.93	156.41	9.89	2.02	−1.89
C_3	8.95	156.18	12.54	4.57	−1.85	8.94	156.22	11.63	6.30	−1.90
TS($B_1 \rightarrow B_2$)	8.92	151.10	93.36	2.92	−2.16					
TS($B_1 \rightarrow B_3$)	9.73	151.74	90.68	2.31	−5.25					
TS($C_1 \rightarrow B_1$)	8.32	155.96	10.80	3.22	4.15					
TS($C_1 \rightarrow C_2$)	8.84	151.44	86.43	0.67	−1.16					
TS($C_1 \rightarrow C_3$)	8.97	150.80	90.08	4.13	−2.62					
TS($B_2 \rightarrow C_2$)	8.50	156.07	18.16	3.87	2.27					
TS($B_3 \rightarrow C_3$)	8.56	155.92	17.03	4.77	1.49					

[a] $\Delta G = \Delta H - T\Delta S$; H=$E_0$+ZPE+H−$H_0$
[b] All energy terms in kcal mol^{-1}

Fig. 3 Optimized transition state geometries at the B3LYP/6-31G* level in gas phase

TS (A₁-A₂)

TS (C₁-B₁)   TS (B₁-B₂)   TS (B₁-B₃)

TS (C₁-C₂)   TS (C₁-C₃)

TS (B₂-C₂)   TS (B₃-C₃)
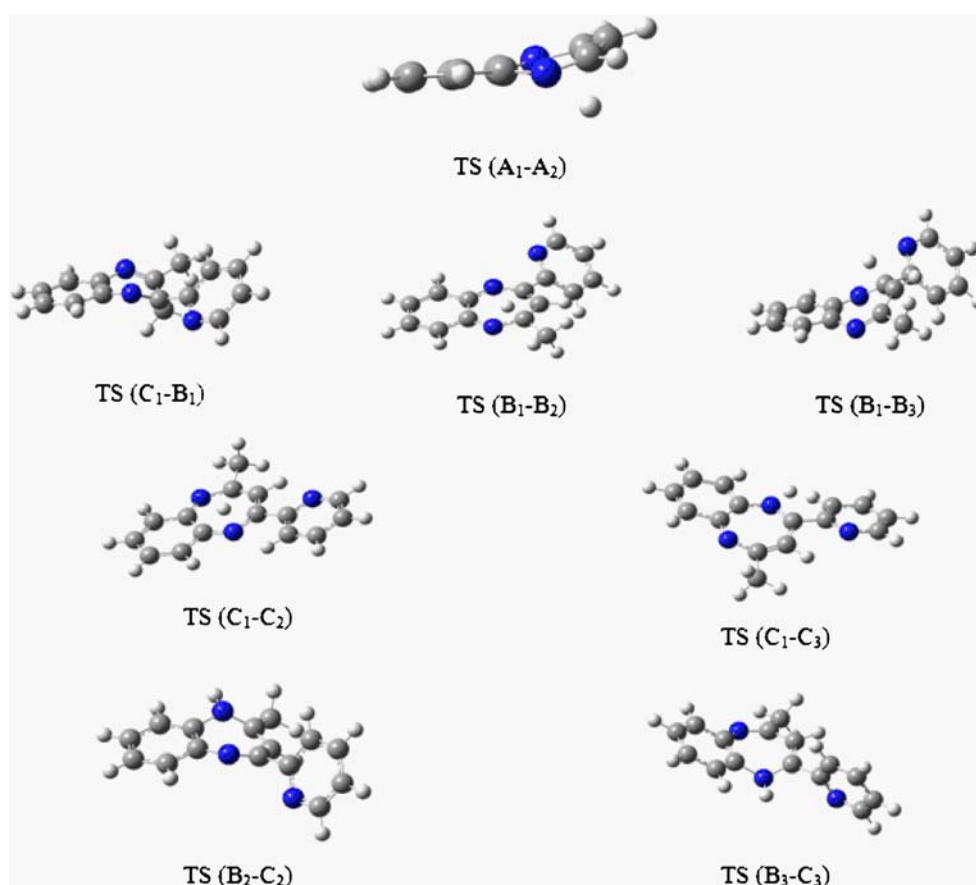
molecules are shown in Fig. 2. The structures drawn here specify the orientation of the bonds and the conformation of the ring in the carbon and hetero atom skeleton.

The analysis of the BZD ring by calculated parameters has shown that the conformations of the **B** and **C** series are very similar to the structures of A_1 and A_2. The computed relevant torsion angle for $C_{10}C_{11}N_5C_4$ was $-37.68°(38.03°$ $\varepsilon=78.54)$ and that for $C_{11}C_{10}N_1C_2$ was $37.38°(38.03°$ $\varepsilon=78.54$) in A_1 while the corresponding angles were $-37.38°$ $(-37.87°$ $\varepsilon=78.54)$ and $37.91°(38.02°$ $\varepsilon=78.54)$ in B_1. This means that the boat conformation of the diazepine ring was not changed by the attachment of substituents. The same angles were also found to be $C_{10}C_{11}N_5C_4=-28.54°$ $(-27.10°$ $\varepsilon=78.54)$ and $C_{11}C_{10}N_1C_2=39.99°(37.61°$ $\varepsilon=$ $78.54)$ for A_2, and $C_{10}C_{11}N_5C_4=-34.24°(-34.61°$ $\varepsilon=78.54)$ and $C_{11}C_{10}N_1C_2=51.77°(51.53°$ $\varepsilon=78.54)$ for B_2. A previous experimental study on the 1,4-BZD derivative molecule thionordazepam [27] showed that the seven-membered ring had a boat conformation with a 66.11° dihedral angle. The $C_2C_3C_4N_5$ angle values ranged from 69.19° to 69.89° in the gas phase and in water. As a result, the agreement between the calculated geometrical parameters and experimental findings for thionordazepam was less good.

The effects on the diazepine ring of piridyl and methyl groups are examined below. One of the most striking structural features of B_1 was the decrease in N_5–C_{11} and C_{10}–N_1 bond lengths; the decreases in bond lengths were N_5–C_{11} 0.008 Å (0.007 Å in water) and C_{10}–N_1 0.002 Å (0.002 Å in water). It should be noted that the decrease in the N_5–C_{11} bond length was larger than that for the C_{10}–N_1 bond, whereas the N_1–C_2, C_2–C_3, C_3–C_4 and C_4–N_5 distances became longer. The increments in bond lengths were: "double bond" N_1–C_2 0.005 Å (0.005 Å in water), "single bonds" C_2–C_3 0.005 Å (0.005 Å in water), C_3–C_4 0.008 Å (0.008 Å in water) and "double bond" C_4–N_5 0.007 Å (0.007 Å in water). In the tautomer B_2, "single bond" N_5–C_{11} decreased by 0.013 Å (0.014 Å in water), while "single bonds" N_1–C_{10} increased by 0.002 Å (0.001 Å in water). These findings require that the N_5–C_{11} single bond assumes a more double bond character, while the N_5–C_4 bond, which is conjugated with π-electrons from the neighboring pyridine ring, assumes a more single bond character. These data are an indication of the delocalization around the $N_2'C_1'C_4N_5$ skeleton in B_1 and B_2. The increments in other bond distances of the diazepine ring were: N_1–C_2 0.017 Å (0.021 Å in water), C_2–C_3 0.002 Å (0.001 Å in water), C_3–C_4 0.011 Å (0.013 Å in water) and

Fig. 4 B3LYP/6-31G* calculated relative stabilities (in kcal mol^{-1}) of the tautomers and rotamers; barriers of tautomerization and rotation in the gas phase of benzodiazepine (BZD) and-methyl-4-pyridin-2′-yl-1,5-benzodiazepine
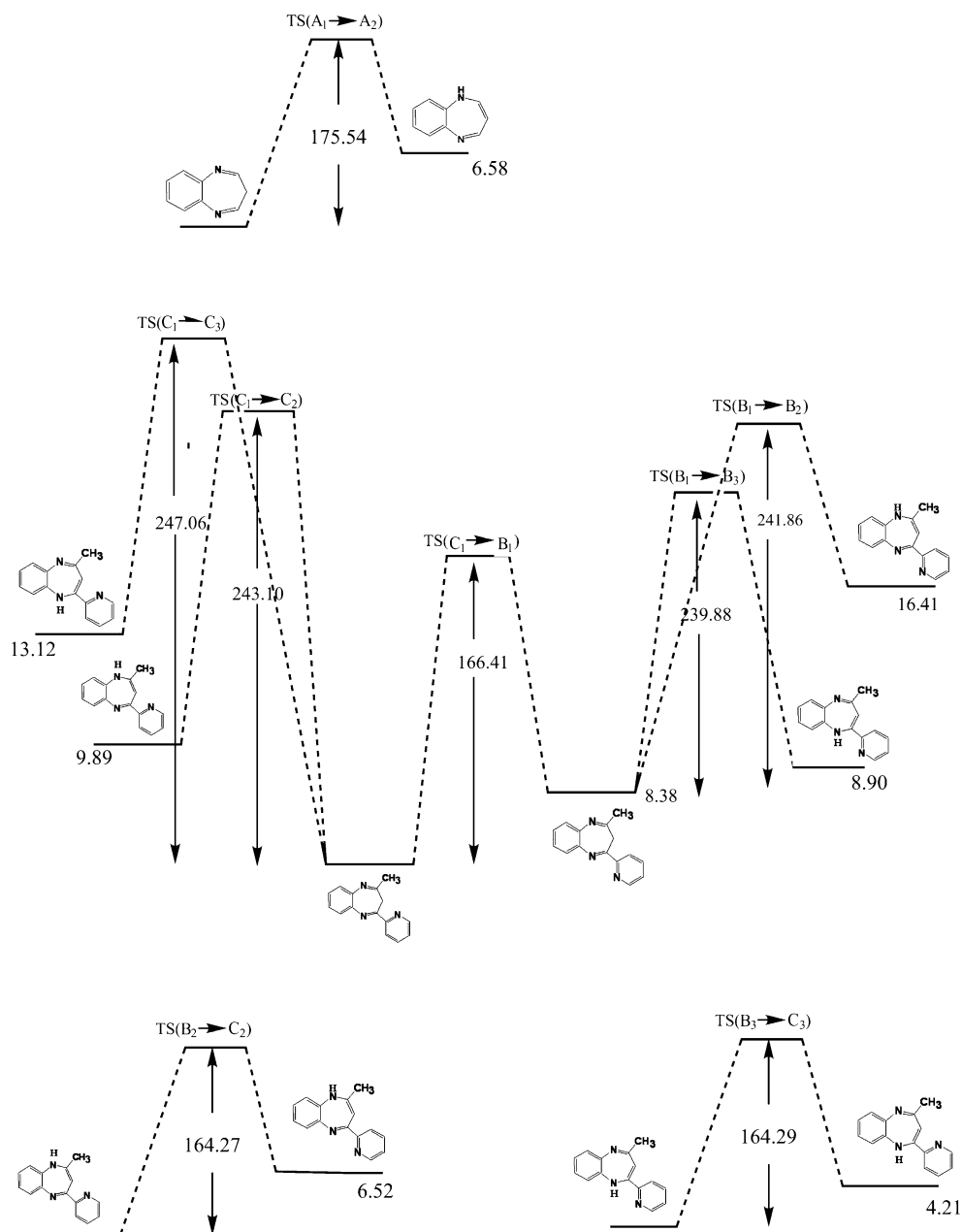
C$_4$–N$_5$ 0.004 Å (0.004 Å in water). In this tautomer, the increase in bond length was greater in the single bond.

Several geometric parameters comparing **B** and **C** tautomers are discussed below. The overall molecular conformation was described by the rotation about the C$_4$–C$_1$′ bond, the torsion angle C$_5$C$_4$C$_1$′N$_2$′ ranged from 8.00° to 33.28° for **B$_1$**, **B$_2$**, **B$_3$** tautomers, and from 155.38° to −176.12° for **C$_1$**, **C$_2$**, **C$_3$** tautomers, in the gas phase and in water.

Although the calculated N–H bond length in **B$_2$** and **C$_2$** is the same, in **C3** this bond length is 0.007 Å shorter than in **B$_3$**. The difference in bond length between **B$_3$** and **C$_3$**

conformers may be due to an intramolecular N–H···N hydrogen bond in the **B$_3$** structure. The greatest change was the shortening of the C$_2$–C$_3$ and C$_3$–C$_4$ bonds and the lengthening of the N$_1$–C$_2$ and N$_5$–C$_4$ bonds when hydrogen was transferred from C$_3$ to N$_{1,5}$. The C$_3$–Ha bond was found to be shorter than the C$_3$–Hb by 0.008 Å and 0.009 Å for **B$_1$** and **C$_1$**, respectively, in the gas phase and in water. This difference is accordance with the value of the **A$_1$** structure.

The results of the calculated total atomic charges are shown in Table 2. Mulliken population analysis indicated that the hetereo atoms N$_1$,N$_5$ and C$_3$ acquired negative charges in all tautomers. It can be seen in Scheme 1 that the

pyridine nitrogen is different positions at B_1 and C_1. According to the position of pyridine nitrogen, the charge distribution changes on the all atoms of the diazepine ring. This is an expected result because of repulsion of the electron pair on the pyridine nitrogen.

Energies

The calculated total energies of the tautomers and rotamers is given in Table 3. The differences in the energies for the species studied are listed in Table 4. The energy difference between the tautomers was not strongly affected by inclusion of higher-order correlation effects. In fact, these energy differences were nearly the same at the HF and B3LYP levels. The most stable A_1 and C_1 structures were taken as reference to obtain the relative energetic stability of tautomers. The free energy difference between two tautomers, ΔG, was obtained by correcting ΔE with the zero-point vibrational energy difference, ΔZPE, the thermal correction difference, $\Delta(H-H_0)$ and the entropy difference, ΔS. All of these correction terms were calculated using the HF/6-31G* and B3LYP/6-31G* optimized geometries and are given in Table 5. The transition state geometries between tautomers and rotamers are given in Fig. 3 and their relatives in Fig. 4. The fused ring of the transition structures had an almost planar geometry.

The shifting hydrogen atom was close to N and far from C_3. Proton transfer from C_3 to $N_{1,5}$ cannot easily occur because the $C_3...N_{1,5}$ distance (2.52–2.58 Å) is too long. The classical barrier heights for proton transfer are very high and tautomerizations proceed very slowly.

As can be seen from the calculated total and relative energy values (Tables 3, 4) the HF and B3LYP methods suggest that the tautomer C_1 was the most stable structure and its rotamer B_1 was the second most stable in the gas phase. The gas phase calculation indicated that the reactions have electronic endothermicity and high energy barriers. The tautomer C_1 was about 10.16 and 9.89 kcal mol^{-1} more stable than the tautomer C_2 in the gas phase, 10.74 and 10.27 kcal mol^{-1} in water, in HF/6-31G* and B3LYP/6-31G* methods, respectively. The C_1 tautomer is also more stable than C_3. These values are much greater than that of the energy differences of the corresponding rotational isomers (Table 3). The large value of the relative energies of these transition states prevent transformation between the different tautomers.

The calculated Gibbs free energy and relative electronic energy values for B_1 and B_2 were greater than the corresponding values for conformers C_1 and C_2, respectively, while conformer C_3 was less stable than B_3. The hydrogen bonds between the pyridine nitrogen and diazepine N–H hydrogen atoms contribute to the stabilization of

B_3. The conformer C_3 has no hydrogen bond. With all processes, calculated high relative energies indicated that the N–H form of the tautomers are more unstable structures than the C–H forms.

The ZPE values of the different conformers are approximately equivalent, so the ZPE contribution to electronic energy changes can be neglected for different conformers. The relative free energy order was found to be $C_3>C_2>C_1$ and also $B_3>B_2>B_1$ in the gas phase. The obtained relative energy order was the same. The SCRF calculations indicated that relative energy order of the tautomers in the gas phase was the same. The tautomer B_3 and its conformer C_3 became more energetically stable than the others in water. The calculated dipole moments are presented in Table 5. The effect of solvent increases the dipole moments of all structures. The results showed that B_3 and C_3 had the largest dipole moments in the gas phase and in water. The dipole moment of B_3 was 5.28 D and 4.96 D at HF/6-31G* and B3LYP/6-31G*, respectively. For the conformer C_3, these dipole moment values were 4.85 D and 4.57 D in the gas phase. For the most stable conformer in the gas phase, C_1, the dipole moment was 3.05 D at HF/6-31G* and 2.56 D at the B3LYP/6-31G* level. It can be seen that B_3 and C_3 were stabilized by 2.06 kcal mol^{-1} (HF), 1.93 kcal mol^{-1} (B3LYP) and 1.82 kcal mol^{-1} (HF), 1.51 kcal mol^{-1} (B3LYP), respectively, in liquid phase. C_1 was stabilized only by 0.71 kcal mol^{-1} (HF), 0.56 kcal mol^{-1} (B3LYP).

Conclusion

In the present study, the structural and energetic characteristic of tautomeric forms of 1,5-benzodiazepine and its 2-methyl-4-pyridin-2′-yl derivative were investigated by ab initio and DFT calculations in the gas phase and in water for the first time. The results indicated that A_1, B_1, and C_1 were the most stable structures in the gas phase and in water. The relative free energy order was found to be $C_3>C_2>C_1$ and also $B_3>B_2>B_1$ in the gas phase and in water. The 5-H tautomer, B_3, was more stable than the C_3 structure due to the hydrogen bond between the pyridine nitrogen and the diazepine N–H hydrogen atom. The C–H form of the tautomers was more stable than the N–H form, and all of the proton transfer processes showed endothermicity and high energy barriers. The boat conformation of the diazepine ring was dominant for all species even with different double bond positions and including substituents. The methylene hydrogens exhibited anisochrony.

References

1. Llyod D, McNab H (1998) Adv Heterocycl Chem 71:1–56
2. Katritzky AR, Abonia R, Yang B, Qi M (1998) Insuasty B. Synthesis-Stuttgart 1487–1490
3. Landguist J K (1984) In Katritzky AR, Rees CW (eds) Comprehensive heterocyclic chemistry, vol 1. Pergamon, Oxford, pp 166–170
4. Fruscella P, Sottocorno M, Di Braccio M, Diomede L, Piccardi N, Cagnotto A, Grossi G, Romano M, Menini T, Roma G (2001) Pharmacol Res 43:445–451
5. Grossi G, Di Braccio M, Roma G, Ballabeni V, Tognolini M, Calcina F, Barocelli E (2002) Eur J Med Chem 37:933–944
6. Randall LO, Kappel B (1973) Pharmacological study of some benzodiazepines and their metabolites. In:Garattini S, Mussini E, Randall LO (eds) The benzodiazepines. Raven, New York, pp 27–52
7. Haris RC, Straley JM (1968) US. Patent 1, 537,757, Chem Abstr (1970) 73 1000 54w
8. Essaber M, Bauid A, Hasnaoui A, Benharref A, Lavergne JP (1998) Synth Commun 28:4097–4104
9. El-Sayed AM, Abdel-Ghany H, El-Saghier AMM (1999) Synth Commun 29:3561–3572
10. Reddy KVV, Rao PS, Ashok D (2000) Synth Commun 30:1825–1836
11. Hegedus A, Hell Z, Pator A (2005) Catalysis Lett 105:229–232
12. Curini M, Epifano F, Marcotullio MC, Rosati O (2001) Tetrahedron Lett 42:3193–3195
13. Jarikote DV, Siddigui SA, Rajagopal R, Daniel T, Lahoti RJ, Srinivason KV (2003) Tetrahedron Lett 44:1835–1838
14. Balakrishna MS, Kaboudin B (2001) Tetrahedron Lett 42:1127–1129
15. Chari MA, Syamasundar KC (2005) Catalysis Commun 6:67–70
16. Nawrocka W, Sztuba B, Opolski A, Wietrzyk J, Kowalska MW, Gowiak T (2001) Synthesis and antiproliferative activity in vitro of novel 1,5-benzodiazepines. Part II. Arch Pharm Pharm Med Chem 334:3–10
17. Pozarentzi M, Stephanidou-Stephanatou J, Tsoleridis CA (2002) Tetrahedron Lett 43:1755–1758
18. Zavala F (1997) Pharmacol Ther 75:199–216
19. Krueger KE, Papadopoulus V (1992) Annu Rev Pharmacol Toxicol 32:211–237
20. Sacerdote P, Panerai AE, Frattola L (1999) Psychoneuroendocrinology 24:243–249
21. Tjiou EM, Lhoussaine EG, Virieux D, Fruchier A (2005) Magn Reson Chem 43:557–562
22. Frisch MJ, Trucks GW, Schlegel HB, Scuseria GE, Robb MA, Cheeseman JR, Montgomery Jr JA, Vreven T, Kudin KN, Burant JC, Millam JM, Iyengar SS, Tomasi J, Barone V, Mennucci B, Cossi M, Scalmani G, Rega N, Petersson GA, Nakatsuji H, Hada M, Ehara M, Toyota K, Fukuda R, Hasegawa J, Ishida M, Nakajima T, Honda Y, Kitao O, Nakai H, Klene M, Li X, Knox JE, Hratchian HP, Cross JB, Bakken V, Adamo C, Jaramillo J, Gomperts R, Stratmann RE, Yazyev O, Austin AJ, Cammi R, Pomelli C, Ochterski JW, Ayala PY, Morokuma K, Voth GA, Salvador P, Dannenberg JJ, Zakrzewski VG, Dapprich S, Daniels AD, Strain MC, Farkas O, Malick DK, Rabuck AD, Raghavachari K, Foresman JB, Ortiz JV, Cui Q, Baboul AG, Clifford S, Cioslowski J, Stefanov BB, Liu G, Liashenko A, Piskorz P, Komaromi I, Martin RL, Fox DJ, Keith T, Al-Laham MA, Peng CY, Nanayakkara A, Challacombe M, Gill PMW, Johnson B, Chen W, Wong MW, Gonzalez C, Pople JA (2003) Gaussian 03. Revision B.04, Gaussian, Pittsburgh PA
23. Onsager L (1936) J Chem Soc 58:1486–1493
24. Dennington II R, Keith T, Millam J, Eppinnett K, Hovell WL, Gilliland R (2003) GaussView, version 3.09. Semichem, Shawnee Mission, KS
25. Walkinshaw MD (1985) Acta Cryst C41:1253–1255
26. Torres H, Insuasty B, Cobo JN, Glidewell C (2005) Acta Cryst C61:404–407
27. Narasegowda RS, Vijay T, Yathirajan HS, et al (2005) Acta Crystallographica Section E-Structure Reports Online 61: O2934–O2936 Part 9